LETTER

Slower recovery in space before collapse of connected populations

Lei Dai[1], Kirill S. Korolev[1] & Jeff Gore[1]

Slower recovery from perturbations near a tipping point and its indirect signatures in fluctuation patterns have been suggested to foreshadow catastrophes in a wide variety of systems[1,2]. Recent studies of populations in the field and in the laboratory have used time-series data to confirm some of the theoretically predicted early warning indicators, such as an increase in recovery time or in the size and timescale of fluctuations[3–6]. However, the predictive power of temporal warning signals is limited by the demand for long-term observations. Large-scale spatial data are more accessible, but the performance of warning signals in spatially extended systems[7–10] needs to be examined empirically[3,11–13]. Here we use spatially extended yeast populations, an experimental system with a fold bifurcation (tipping point)[6], to evaluate early warning signals based on spatio-temporal fluctuations and to identify a novel spatial warning indicator. We found that two leading indicators based on fluctuations increased before collapse of connected populations; however, the magnitudes of the increases were smaller than those observed in isolated populations, possibly because local variation is reduced by dispersal. Furthermore, we propose a generic indicator based on deterministic spatial patterns, which we call 'recovery length'. As the spatial counterpart of recovery time[14], recovery length is the distance necessary for connected populations to recover from spatial perturbations. In our experiments, recovery length increased substantially before population collapse, suggesting that the spatial scale of recovery can provide a superior warning signal before tipping points in spatially extended systems.

Positive feedback is widespread in nature, ranging from cellular circuits to population growth to the melting of ice sheets. There is growing evidence that positive feedback leads to alternative stable states and tipping points in various ecological systems[15–18]. Closer to a tipping point an ecosystem becomes less resilient and more likely to shift to an alternative state[19] such as the collapse of fish stocks, eutrophication of lakes, or loss of vegetation[20]. Predicting these undesirable transitions may sound like an impossible task because of the inherent complexity underlying these systems. However, recent advances incorporating ideas from nonlinear dynamical systems theory suggest that there may be signatures of "critical slowing down" in the vicinity of tipping points[1,2]. At the brink of these sudden transitions, the recovery of a system after perturbations should slow down[14], also leading to changes in the pattern of fluctuations[21]. Thus, a set of indicators related to critical slowing down may provide advance warning of an impending transition. Empirical tests in the field[4] and in the laboratory[3,5,6] have revealed some of the early warning signals based on fluctuations in time series, such as temporal variation and autocorrelation.

However, our understanding of early warning signals in spatially extended systems is still limited[1,2]. The studies in time series typically ignore spatial interactions; in reality spatial coupling between habitat patches (for example, dispersal of populations or exchange of biomass) is common and may affect the performance of some warning signals[22]. Moreover, temporal warning signals rely on data from long-term observations, which are scarce and difficult to obtain. Large-scale spatial data, such as satellite-derived data sets[17], could be more readily available.

Spatial data not only provide a greater quantity of information, but also allow us to study features of the system that are not available through time series. Statistical indicators based on spatial fluctuations have been proposed[7–10] but empirical studies are limited[3,11,12]; tests of these indicators in replicated experiments, which avoid the bias introduced by selective sampling[23], are lacking. In addition, previous studies of vegetation systems discovered emerging spatial patterns preceding transitions[24,25]. However, the vegetation patterns are often specific to the system studied, whereas identifying generic spatial warning signals would add a powerful tool to the analysis of ecosystem stability. Here we address these questions using an experimental system of spatially extended yeast populations with alternative stable states and a tipping point leading to population collapse.

We grew laboratory populations of the budding yeast *Saccharomyces cerevisiae* in sucrose and performed daily dilution into fresh media. During the daily dilution, a fraction (for example, 1 in 500 for a dilution factor of 500) of the cells were transferred to fresh media. This is a well characterized system with an experimentally mapped fold bifurcation (tipping point)[6]. Yeast cells grow cooperatively in sucrose by sharing the hydrolysis products[26], creating a positive feedback between cells that leads to bistability and a tipping point (Supplementary Fig. 1). By increasing the dilution factor (equivalent to an increase in the mortality rate), we could drive isolated yeast populations to collapse on crossing the tipping point (Fig. 1a).

We then connected local yeast populations spatially through controlled dispersal between nearest neighbours on a one-dimensional array (Fig. 1b). Spatial coupling between local populations was introduced by adding a dispersal step during the daily dilution. In the dispersal step, 25% (corresponding to a dispersal rate $D = 2 \times 25\% = 0.5$) of a local population was transferred to each of its nearest neighbours; the rest of the population remained in the patch. For each dilution factor, there were four replicate arrays each consisting of ten patches. A group of isolated populations ($D = 0$) was grown in a similar experimental setting except that there was no mixing between neighbours (Methods). The isolated populations served as a control group and allowed us to investigate the effects of spatial coupling on warning signals. From dilution factor 500 to 1,600, both groups of connected and isolated populations survived and reached equilibrium densities in a week; at dilution factor 1,700, most of the populations collapsed within the timescale of our experiment (insets to Fig. 1a).

After the populations stabilized, we tracked the fluctuations of population density around equilibrium for at least five days to calculate statistical indicators (Methods). Consistent with critical slowing down, we observed a clear increase in the coefficient of variation (CV) of connected populations towards the tipping point (Fig. 2a); however, the magnitude of increase in CV was smaller than in the isolated populations. We then tested lag-1 autocorrelation, a leading indicator for the temporal correlation of fluctuations. As expected, we found that the temporal correlation of connected populations increased gradually to around 0.6 in the vicinity of the tipping point (Fig. 2b). Similar to the observation in CV, the signal in temporal correlation was weaker than in the isolated populations. Although fluctuations of population density
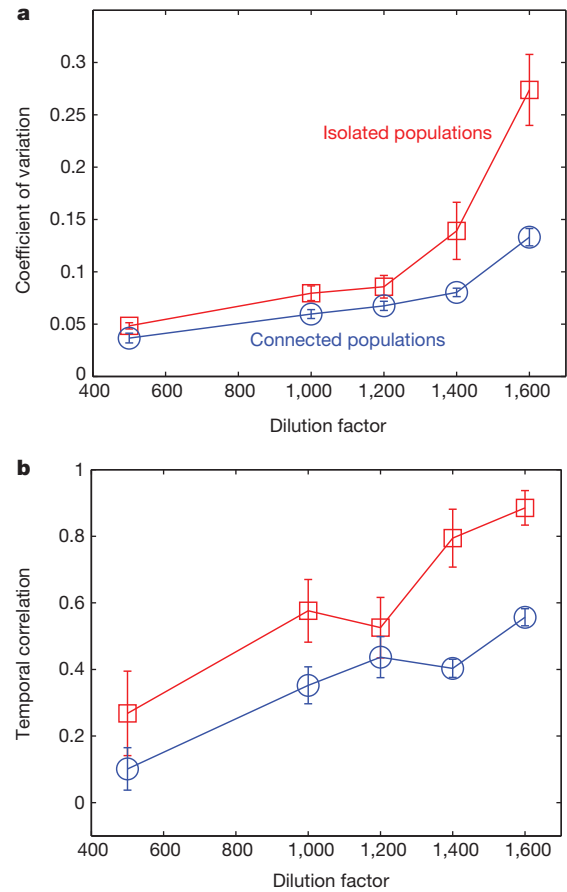
[1]Department of Physics, Massachusetts Institute of Technology, Cambridge, Massachusetts 02139, USA.
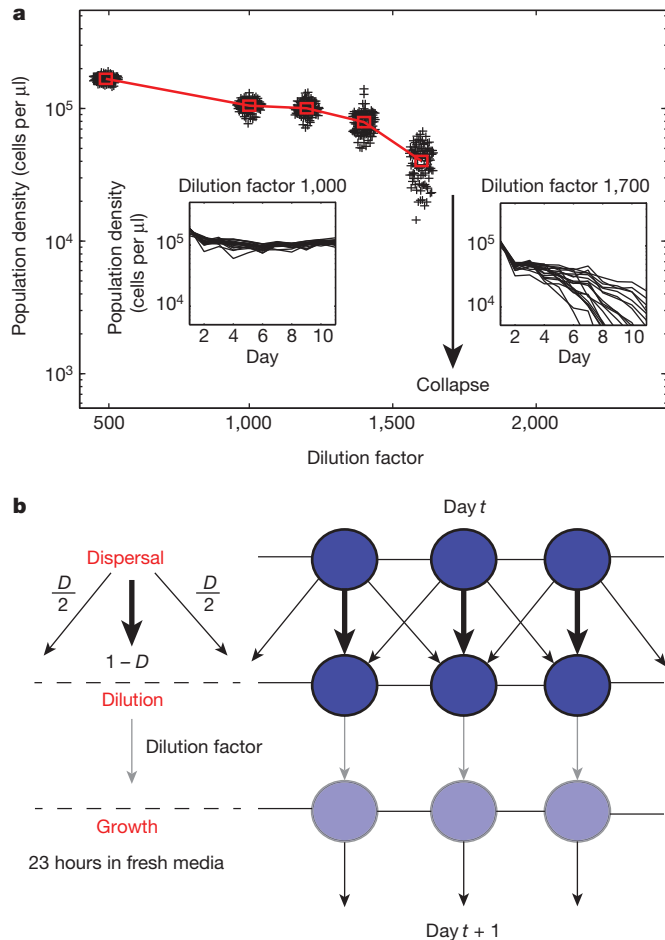
Figure 1 | Yeast populations with a tipping point: an experimental system to study the collapse of connected populations. a, Isolated yeast populations collapse after crossing a tipping point. The distribution of population density around equilibrium is shown in spread points; the red square denotes the mean. Insets are traces of replicate populations at dilution factor 1,000 (stable) and 1,700 (collapsed). **b**, Yeast populations are spatially connected by controlled daily dispersal. Each circle corresponds to a habitat patch where a local population grows. A fraction of the local population is transferred to each of its two nearest neighbours, and the rest to itself.

Figure 2 | Early warning signals based on fluctuations show suppressed increase in connected populations. a, Coefficient of variation (CV). **b**, Temporal correlation (lag-1 autocorrelation). The coefficient of variation and temporal correlation of both isolated populations (red squares) and connected populations (blue circles) increased before the tipping point. The signals were suppressed in the connected populations, possibly owing to the averaging effect of dispersal. Error bars are standard errors given by bootstrap for isolated populations and standard errors of the mean ($n = 4$) for connected populations.

in general became larger and more correlated before population collapse, we found that these two warning signals (CV and lag-1 autocorrelation) seemed to be suppressed in the presence of dispersal, especially at higher dilution factors.

One explanation for the observed suppression of the two leading indicators in connected populations is that flows between neighbours smooth out the fluctuations across different patches and effectively reduce the autocorrelation in any local population. Reduced size or timescale of fluctuations due to dispersal among populations was predicted in previous theoretical studies of spatially explicit ecological models[8,10,22,27]. We note that the smaller warning signals of connected populations in our experiment may be partly due to a minor shift in the tipping point (Supplementary Fig. 2). The averaging effect of dispersal was also found in an independent group of populations subject to '100% dispersal treatment', in which we mixed ten populations completely each day during the dispersal step. In this extreme scenario, the populations showed almost no increase in variation before the tipping point (Supplementary Fig. 3). Moreover, we demonstrated the suppression of CV and lag-1 autocorrelation by dispersal in analytical derivations based on a spatially explicit first-order autoregressive model (Supplementary Note 1) and in stochastic simulations using a phenomenological model of yeast growth[6] (Supplementary Fig. 4).
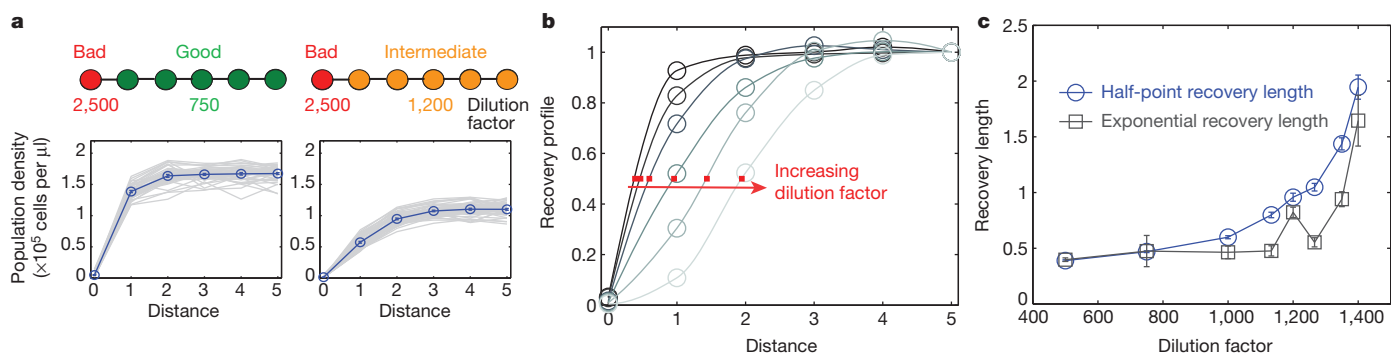
Spatial coupling introduces the possibility of another warning indicator based on spatial fluctuations: spatial correlation. Long-range spatial correlation has been known to occur in the vicinity of some phase transitions[28]; recent theoretical work in spatially explicit ecological models found that increasing spatial correlation could be a warning signal before transitions to an alternative stable state[8]. We tested the two-point correlation between nearest neighbours in the connected populations but failed to observe any increase near the tipping point (Supplementary Fig. 5). Simulation results with varying sample size showed that no statistically significant increase in spatial correlation should be discerned with the limited samples in our experiment. Thus, our results suggest that to observe the increase in spatial correlation may require more data than for other indicators.

Facing the potential difficulty of observing a strong warning signal based on fluctuations in spatially connected populations, we set out to look for possible new indicators. The existing warning signals can be classified into different categories, based on the nature of the perturbations and measurements (see Fig. 3). Measuring the recovery time after a pulse perturbation (Fig. 3a) can provide a robust indicator of the distance to a tipping point[5,14]. In large complex systems, it is often impractical to perform such temporal perturbations repeatedly and measure recovery time. However, owing to stochastic perturbations such as demographic noise, population density constantly fluctuates around the equilibrium. Changes of fluctuation patterns such as an
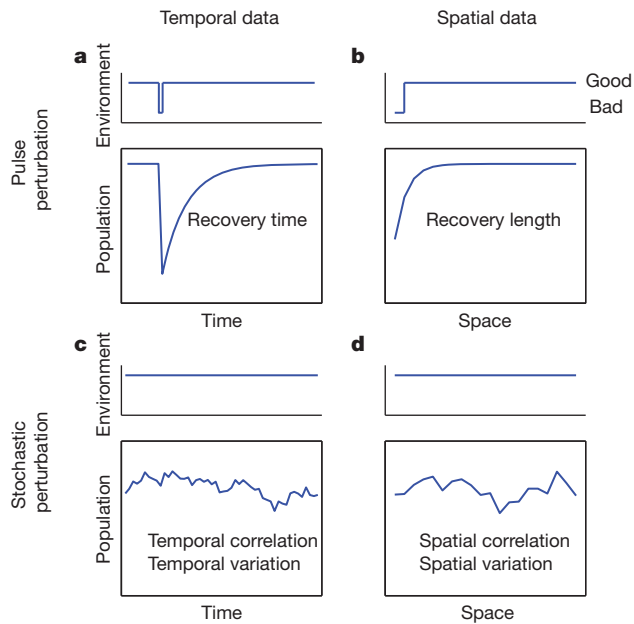
Figure 3 | Early warning signals can be classified into four categories by the nature of perturbations and measurements. a, Recovery time; **b**, Recovery length; **c**, Statistical indicators based on temporal fluctuations; **d**, Statistical indicators based on spatial fluctuations. The unexplored category of early warning signals is the spatial counterpart of recovery time: 'recovery length'. The recovery length characterizes the spatial scale over which population density recovers from a pulse perturbation in space, such as at a boundary with a region of lower quality (**b**). The recovery length increases towards the tipping point (Supplementary Note 2) and provides a novel indicator of critical slowing down in spatial data.

increase in variation and correlation (Fig. 3c, d), measured either in time or in space, are also signatures of critical slowing down and consist of another two categories of leading warning signals[3,4,6–10,21]. Surprisingly, there is one remaining category that has not been proposed: find or create a 'pulse perturbation in space' (Fig. 3b) and measure the spatial counterpart of recovery time[14]. Adjacent to a region of poor quality, the neighbouring good patches will not immediately have reached their carrying capacity; instead the carrying capacity will be reached only further from the bad region (Supplementary Fig. 6). Rather than an increase in the timescale to recover, critical slowing down here manifests itself as an increase in the spatial scale to recover (Supplementary Note 2), that is, an increase in 'recovery length' as compared to 'recovery time'.

To test our 'recovery length' hypothesis, we performed another set of experiments with spatially connected yeast populations (dispersal rate $D = 0.5$), now with two different regions: a relatively good (lower dilution factor) region of five patches and a bad (high dilution factor) region of one patch (Fig. 4a). Given this sharp boundary between two regions of different quality, population density in the good region recovered gradually in space to the equilibrium value. As the condition of the good region deteriorates, we expect an increase in the spatial scale over which the populations recover. Indeed, we observed a clear change in the steady-state recovery profile of populations with increasing dilution factor of the good region (Fig. 4b). In agreement with our hypothesis, the spatial recovery spanned a much longer distance closer to the tipping point.

We quantified this spatial scale using two different indicators (Fig. 4c). The first indicator, the 'half-point recovery length', measures the distance between the bad region and the location of half recovery (Methods). The half-point recovery length increased gradually with dilution factor from less than 0.5 to around 2. The second indicator, the 'exponential recovery length', is obtained by fitting the recovery profile with an exponential function (Methods). Similar to the first indicator, the exponential recovery length increased more than three-fold as the tipping point was approached. Thus, both measures suggest that the recovery length provides a strong warning signal before population collapse in our system. We also observed an increase in both indicators as we slowly caused the good region to deteriorate by increasing the dilution factor and induced the collapse of connected populations in real time (Supplementary Fig. 7).

Recovery length completes the four categories of early warning signals and can help improve our assessment of spatially extended systems. Our results suggest that stronger spatial coupling (higher dispersal rate) suppresses early warning signals in CV and temporal correlation (Supplementary Fig. 4). In contrast, the magnitude of recovery length increases with the level of spatial coupling (Supplementary Note 2). These two categories of early warning signals are therefore complementary: when one signal is weak the other is strong. Also, although our experiment was conducted on a linear array, the use of recovery length can be readily generalized to two-dimensional systems by mapping the profile perpendicularly to contours of population density. Unlike the specific spatial patterns found in two-dimensional vegetation systems[24,25], recovery length may provide a generic measure given that the spatially coupled units by themselves would recover more slowly near the tipping point.

Finally, from a practical perspective, boundaries between regions of different quality are ubiquitous in nature, thus providing many opportunities to measure the recovery length in populations of interest. One specific example of recovery length would be the "distance of

Figure 4 | Recovery length provides a direct measure of critical slowing down in space. a, Connected populations in relatively good regions of dilution factor 750 (left) and 1,200 (right) recover gradually in space to the equilibrium density. Blue circles denote the steady-state profile of population density after averaging over replicates (shown in grey). **b**, Recovery profiles at dilution factor 500, 750, 1,000, 1,200, 1,350 and 1,400 show an increasing spatial scale of

recovery. The profile is normalized by the population density of the patch furthest from the bad region. Lines are shape-preserving interpolations; the position of half-recovery is marked by a red square. **c**, Two different measures of recovery length increase substantially with dilution factor. Error bars are standard errors given by bootstrap.

edge influence" in landscape ecology[29]: it quantifies the spatial scale of edge influence on biota in fragmented landscapes. Data of edge influence for forests at different sites suggest a longer recovery length in the Australian tropical forests[30], which seems to be borne out by the recent forest collapses in Western Australia. In principle, the recovery length can also be measured when spatially extended populations 'recover' from a region of higher quality (Supplementary Figs 6 and 8), suggesting that boundaries may be introduced by conservation efforts (for example, setting up marine reserves).

Our experiments were performed in the simplest spatial setting possible: homogeneous environments and dispersal rates, a large population size and a safe distance away from the tipping point. In the presence of environmental heterogeneity, measurement of recovery length may fail if the desired sharp boundary between regions of different quality is blurred. However, in such a case we would expect enhanced signals in spatial correlation[8] and spatial variation before population collapse (Supplementary Fig. 9). Our experiments have also not explored the effects of spatial coupling on the global stability of a meta-population. On the one hand, spatial coupling may reduce fluctuations and the probability that a random shock will trigger a state shift[22]; on the other hand, stochastic local extinctions or the introduction of a bad region may drive the connected populations to collapse before the tipping point of a local population (Supplementary Note 3).

Our work illustrates the important role of spatial coupling, such as the dispersal of populations, in our understanding of how to apply the current toolbox of warning indicators to natural populations. More empirical studies are required to confirm the generality and applicability of different indicators, but being able to observe warning signals in connected populations suggests that we may be able to develop quantitative metrics for assessing the fragility of spatially extended complex systems.

METHODS SUMMARY

We grew the budding yeast *Saccharomyces cerevisiae* in 200 μl batch culture on BD Falcon 96-well Microtest plates at 30.7 °C (±0.2 °C, standard deviation) using synthetic media supplemented with 2% sucrose[6]. Serial dilutions were performed daily with variable dilution factors. Population densities were recorded each day before the serial dilution by measuring optical density at 600 nm. Statistical indicators were calculated after the populations stabilized. The coefficient of variation was calculated as the sample standard deviation divided by the sample mean. The temporal correlation was estimated by the Pearson's correlation coefficient between the population densities at subsequent days. In the experiment to measure recovery length, the half-point recovery length was estimated by performing a shape-preserving interpolation to the steady-state recovery profile of population density and then locating the position of half-recovery. The exponential recovery length was estimated by fitting an exponential function to the recovery profile. For further details, see the online-only Methods.

Full Methods and any associated references are available in the online version of the paper.

1. Scheffer, M. *et al.* Early-warning signals for critical transitions. *Nature* **461,** 53–59 (2009).
2. Scheffer, M. *et al.* Anticipating critical transitions. *Science* **338,** 344–348 (2012).
3. Drake, J. M. & Griffen, B. D. Early warning signals of extinction in deteriorating environments. *Nature* **467,** 456–459 (2010).
4. Carpenter, S. R. *et al.* Early warnings of regime shifts: a whole-ecosystem experiment. *Science* **332,** 1079–1082 (2011).
5. Veraart, A. J. *et al.* Recovery rates reflect distance to a tipping point in a living system. *Nature* **481,** 357–359 (2012).
6. Dai, L., Vorselen, D., Korolev, K. S. & Gore, J. Generic indicators for loss of resilience before a tipping point leading to population collapse. *Science* **336,** 1175–1177 (2012).
7. Guttal, V. & Jayaprakash, C. Spatial variance and spatial skewness: leading indicators of regime shifts in spatial ecological systems. *Theor. Ecol.* **2,** 3–12 (2009).
8. Dakos, V., Nes, E. H., Donangelo, R., Fort, H. & Scheffer, M. Spatial correlation as leading indicator of catastrophic shifts. *Theor. Ecol.* **3,** 163–174 (2010).
9. Dakos, V., Kéfi, S., Rietkerk, M., Van Nes, E. H. & Scheffer, M. Slowing down in spatially patterned ecosystems at the brink of collapse. *Am. Nat.* **177,** E153–E166 (2011).
10. Carpenter, S. R. & Brock, W. A. Early warnings of regime shifts in spatial dynamics using the discrete Fourier transform. *Ecosphere* **1,** art10 (2010).
11. Lindegren, M. *et al.* Early detection of ecosystem regime shifts: a multiple method evaluation for management application. *PLoS ONE* **7,** e38410 (2012).
12. Litzow, M. A., Urban, J. D. & Laurel, B. J. Increased spatial variance accompanies reorganization of two continental shelf ecosystems. *Ecol. Appl.* **18,** 1331–1337 (2008).
13. Ouyang, Q. & Swinney, H. L. Transition from a uniform state to hexagonal and striped Turing patterns. *Nature* **352,** 610–612 (1991).
14. van Nes, E. H. & Scheffer, M. Slow recovery from perturbations as a generic indicator of a nearby catastrophic shift. *Am. Nat.* **169,** 738–747 (2007).
15. May, R. M. Thresholds and breakpoints in ecosystems with a multiplicity of stable states. *Nature* **269,** 471–477 (1977).
16. Scheffer, M., Carpenter, S. & Foley, J. A. Folke, C. & Walker, B. Catastrophic shifts in ecosystems. *Nature* **413,** 591–596 (2001).
17. Staver, A. C., Archibald, S. & Levin, S. A. The global extent and determinants of savanna and forest as alternative biome states. *Science* **334,** 230–232 (2011).
18. Isbell, F., Tilman, D., Polasky, S., Binder, S. & Hawthorne, P. Low biodiversity state persists two decades after cessation of nutrient enrichment. *Ecol. Lett.* http://dx.doi.org/10.1111/ele.12066 (2013).
19. Holling, C. S. Resilience and stability of ecological systems. *Annu. Rev. Ecol. Syst.* **4,** 1–23 (1973).
20. Scheffer, M. *Critical Transitions in Nature and Society* (Princeton Univ. Press, 2009).
21. Kleinen, T., Held, H. & Petschel-Held, G. The potential role of spectral properties in detecting thresholds in the Earth system: application to the thermohaline circulation. *Ocean Dyn.* **53,** 53–63 (2003).
22. Brock, W. A. & Carpenter, S. R. Interacting regime shifts in ecosystems: implication for early warnings. *Ecol. Monogr.* **80,** 353–367 (2010).
23. Boettiger, C. & Hastings, A. Early warning signals and the prosecutor's fallacy. *Proc. R. Soc. Lond. B* **279,** 4734–4739 (2012).
24. Rietkerk, M., Dekker, S. C., De Ruiter, P. C. & Van de Koppel, J. Self-organized patchiness and catastrophic shifts in ecosystems. *Science* **305,** 1926–1929 (2004).
25. Kéfi, S. *et al.* Spatial vegetation patterns and imminent desertification in Mediterranean arid ecosystems. *Nature* **449,** 213–217 (2007).
26. Gore, J., Youk, H. & Van Oudenaarden, A. Snowdrift game dynamics and facultative cheating in yeast. *Nature* **459,** 253–256 (2009).
27. Fernández, A. & Fort, H. Catastrophic phase transitions and early warnings in a spatial ecological model. *J. Stat. Mech.* P09014 (2009).
28. Sole, R. V., Manrubia, S. C., Luque, B., Delgado, J. & Bascompte, J. Phase transitions and complex systems. *Complexity* **1,** 13–26 (1996).
29. Ries, L., Fletcher, R. J., Battin, J. & Sisk, T. D. Ecological responses to habitat edges: mechanisms, models, and variability explained. *Annu. Rev. Ecol. Evol. Syst.* **35,** 491–522 (2004).
30. Harper, K. A. *et al.* Edge influence on forest structure and composition in fragmented landscapes. *Conserv. Biol.* **19,** 768–782 (2005).

Author Contributions L.D., K.S.K. and J.G. designed the study. L.D. performed the experiments and analysis. K.S.K. and J.G. assisted with the analysis. L.D., K.S.K. and J.G. wrote the manuscript.

Author Information Reprints and permissions information is available at www.nature.com/reprints. The authors declare no competing financial interests. Readers are welcome to comment on the online version of the paper. Correspondence and requests for materials should be addressed to L.D. (dailei@mit.edu) or J.G. (gore@mit.edu).

METHODS

Experimental protocols. We grew the budding yeast *Saccharomyces cerevisiae* in 200 μl batch culture on BD Falcon 96-well Microtest plates at 30.7 °C (±0.2 °C, standard deviation) using synthetic media (yeast nitrogen bases + nitrogen, Complete Supplement Mixture) supplemented with 2% sucrose[6]. Cultures were maintained in a well-mixed condition by growing on a shaker at 825 r.p.m. Serial dilutions were performed daily (23 h of growth) with variable dilution factors. Population densities were recorded each day before the serial dilution by measuring optical density at 600 nm using a Thermo Scientific Varioskan Flash Multimode Reader. The calibration between optical density and cell density was based on the previous characterization of this system[6].

In the group of connected populations, for each dilution factor there were four replicate arrays each consisting of ten patches. Populations were connected by controlled dispersal between nearest neighbours (dispersal rate $D = 0.5$, which is defined as the fraction of population going out of a patch). Reflecting boundary conditions were adopted, meaning that a population on the edge would have 75% of its cells remaining in the patch during the dispersal step. In the group of isolated populations, the experiment was performed in a similar spatial setting except that there was no dispersal ($D = 0$); for each dilution factor there were four arrays each consisting of five patches, giving a total of 20 replicate populations isolated from each other. The dilution factors for the data presented in Fig. 2 are 500, 1,000, 1,200, 1,400 and 1,600. In the experiment to measure recovery length, populations were connected by nearest-neighbour dispersal ($D = 0.5$, reflecting boundary conditions). The dilution factor for the bad region (one patch) was 2,500; the dilution factor for the good region (five patches) was varied as the environmental driver. The dilution factors for the data presented in Fig. 4 are 500, 750, 1,000, 1,133, 1,200, 1,266, 1,350 and 1,400.

Calculation of statistical indicators. Statistical indicators for the connected populations were calculated among ten populations in one array on each day and averaged over a span of at least five days, after the populations stabilized. The mean value of four replicate arrays and the standard error of the mean ($n = 4$) are shown in Fig. 2. For the isolated populations, statistical indicators were calculated on each day among 20 populations over five days. We used bootstrap to compute the standard errors of the indicators by resampling 1,000 times the ensemble of replicate populations (for the coefficient of variation and the temporal correlation) or arrays (for the spatial correlation).

The coefficient of variation (CV) was calculated as the sample standard deviation (Supplementary Fig. 3c) divided by the sample mean. Because the local populations in our experiment were grown in a homogeneous environment, in principle they could all be treated as replicates. Assuming the system is ergodic, the CV calculated over an ensemble of replicates can be interpreted either as the spatial CV of many populations at one time point or the temporal CV of a single population over many time points. The temporal correlation, defined as the lag-1 autocorrelation, was estimated by the Pearson's correlation coefficient between the population densities at subsequent days. To correct for negative bias in small samples, we used a modified estimator with an additional term $1/N$ for lag-1 autocorrelation[31]. The sample size $N = 10$ for connected populations and

$N = 20$ for isolated populations. N is a fixed number for different dilution factors, so using the modified estimators would not affect the trend of indicators. The spatial correlation, defined as the two-point correlation between all neighbouring pairs, was estimated by the Moran's coefficient[8,32]. The expectation of Moran's coefficient is $-1/(N-1)$ in the absence of spatial correlation[33]; we used a modified estimator with an additional term $1/(N-1)$ so that the expectation is 0. In this case, the sample size N is the number of patches in an array: $N = 10$ for connected populations and $N = 5$ for isolated populations. For detailed formulae of the statistical indicators, see Supplementary Note 4.

In the analysis we ensured environmental homogeneity by removing the linear gradient of population density observed in connected populations. This small gradient is presumably caused by some heterogeneity in experimental conditions (temperature, dilution errors, and so on) across the plate. Removing gradient-type spatial heterogeneity before statistical analysis is similar to the detrending procedure commonly used in time-series analysis; it prevents spurious signals such as positive spatial correlation (Supplementary Fig. 10).

Recovery length. After the recovery profile stabilized, we tracked the population density profiles of at least six replicates over several days. The half-point recovery length L_{half} was estimated by performing a shape-preserving interpolation (Matlab function PCHIP, piecewise cubic Hermite interpolating polynomial) to the recovery profile and then locating the position of half-recovery, at which $n(x = L_{half}) = (1/2)n(x = 5)$. The population density of the bad region (dilution factor 2,500) in our experiment was close to 0 (Fig. 4 and Supplementary Fig. 7). In the more general scenario with a sharp boundary between two regions of different quality (Supplementary Figs 6 and 8), the position of half-recovery can be defined as the midpoint between the equilibrium population density of the region of interest and the population density at the boundary.

The exponential recovery length L_{exp} was estimated by fitting an exponential function with three parameters $c_1\exp(-x/L_{exp}) + c_2$ to the recovery profile $n(x)$. The data points used for exponential fitting are from positions 1 to 5 (except for dilution factor 500, the data for fitting are from positions 0 to 5). We note that our definition of exponential recovery length is phenomenological, because: (1) the deviation is expected to be exponential only close enough to the equilibrium; (2) at higher dilution factors the profile can deviate from an exponential form (Supplementary Fig. 11). The 'kink' in the fitted exponential recovery length (Fig. 4c) may be due to the limited data points used in fitting or experimental errors. For both the half-point recovery length and the exponential recovery length, we used bootstrap to compute standard errors for the indicators by resampling the ensemble of steady-state profiles 100 times and fitting the average recovery profile.

31. DeCarlo, L. T. & Tryon, W. W. Estimating and testing autocorrelation with small samples: a comparison of the c-statistic to a modified estimator. *Behav. Res. Ther.* **31,** 781–788 (1993).
32. Legendre, P. & Fortin, M. J. Spatial pattern and ecological analysis. *Vegetatio* **80,** 107–138 (1989).
33. Moran, P. A. P. Notes on continuous stochastic phenomena. *Biometrika* **37,** 17–23 (1950).